JEM

SUPPLEMENTAL MATERIAL

Naik et al., http://www.jem.org/cgi/content/full/jem.20100951/DC1

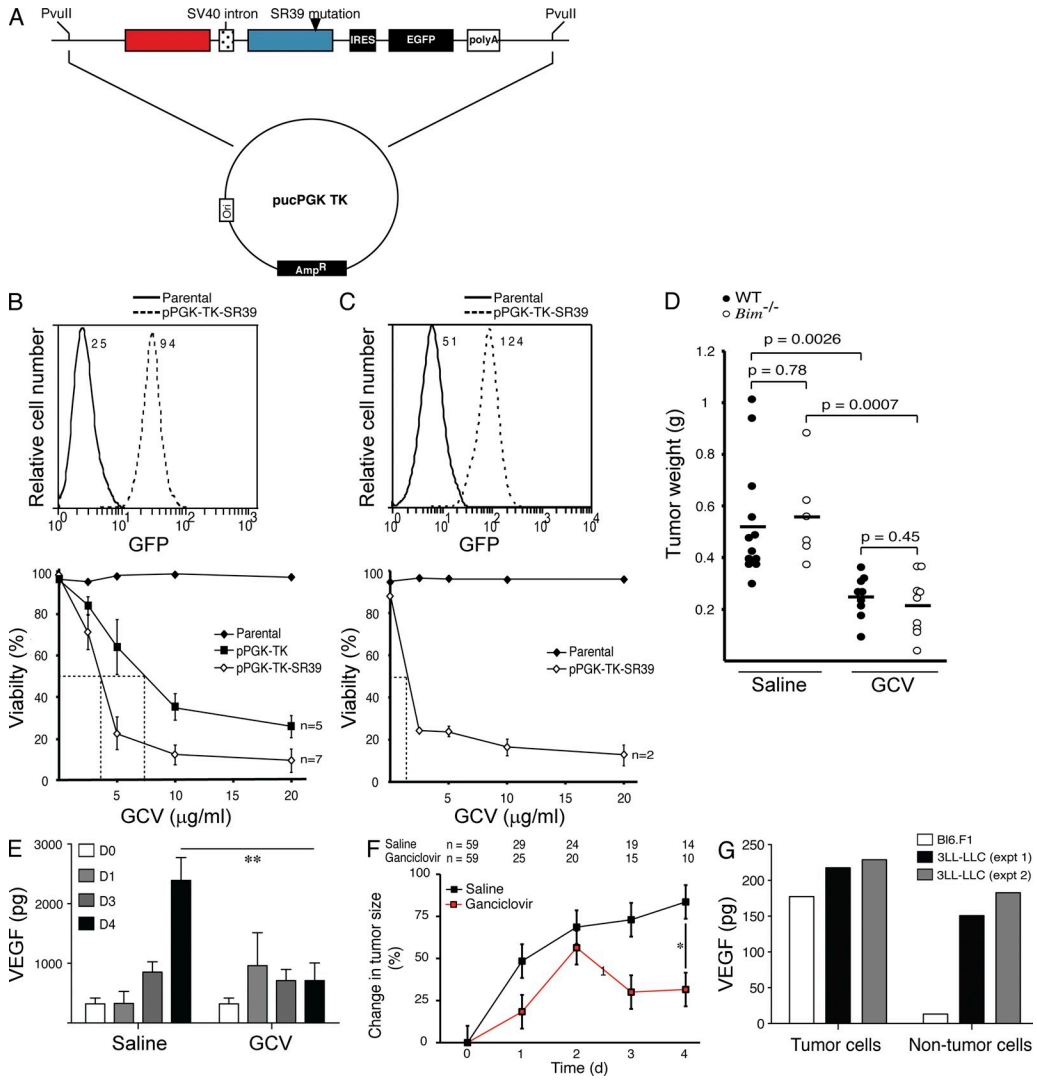

Figure S1. B16.F1 and 3LL-LLC tumor cell lines stably expressing mutant, hyperactive TK (TK-SR39) are killed by GCV treatment in vitro. (A) The construct encoding mutant, hyperactive TK (TK-SR39) from the PGK promoter and EGFP from an IRES (internal ribosomal entry site). (B, top) FACS analysis of GFP expression in one of the TK-SR39 TK-IRES-EGFP vector–transduced B16.F1 clones selected for subsequent in vivo experiments (dashed line). Parental (nontransfected) Bl16.F1 cells were used as a negative control (solid line). Numbers indicate the mean GFP fluorescence intensity. (bottom) B16.F1 cells were treated in vitro with the indicated concentrations of GCV, and cell viability was analyzed 48 h later by PI staining followed by FACS analysis. Data represent mean ± SD (n = 5–7 independent pPGK-TK and pPGK-TK-SR39 clones). The dashed line indicates the dose of GCV that killed 50% of the cells. (C, top) FACS analysis of GFP expression in one of the TK-IRES-EGFP vector–transduced 3LL-LLC clones selected for subsequent in vivo experiments (dashed line). Parental (nontransfected) 3LL-LLC cells were used as a negative control (solid line). Numbers indicate the mean EGFP fluorescence intensity. (bottom) 3LL-LLC cells were treated in vitro with the indicated concentrations of GCV, and cell viability was measured 48 h later by PI staining followed by FACS analysis. Data represent mean ± SD (n = 2 independent pPGK-TK-SR39 clones). The dashed line indicates the dose of GCV that killed 50% of the cells. (D) Saline or GCV treatment was initiated when B16.F1 melanomas growing subcutaneously in WT or $Bim^{-/-}$ mice reached a nominal volume of 50 mm^3. Mice were treated with three daily injections of GCV or saline and harvested on day 4. Horizontal bars indicate mean tumor volume, and each dot represents an independent mouse. Tumors shrink to a similar extent in WT and $Bim^{-/-}$ mice because tumor cell killing and tumor shrinkage at this early time point are a direct consequence of GCV-induced toxicity to tumor cells. Death of intratumoral ECs, which is Bim dependent, affects tumor growth only at a later time point. B16.F1 melanomas were grown in WT mice and treated with GCV or saline as described in Mice, expression constructs, and tumor models. (E and F) The levels of VEGF within tumors (E; expressed as total amount of VEGF per tumor; n = 5 mice per time-point and treatment modality) and tumor volume (F) were measured on days 0–4. Data represent mean ± SEM, and statistical analyses were performed using the Student's t test (*, $P < 0.05$; **, $P < 0.005$). n, number of mice analyzed to determine percent change in tumor size. (G) TK-expressing B16.F1 melanomas and 3LL-LLCs were grown subcutaneously in WT mice, until they reached ∼50 mm^3. Tumors were then harvested, and single-cell suspensions were prepared and then sorted on the basis of GFP expression; live tumor cells GFP^+PI^- and live nontumor (i.e., tumor-associated stromal) cells GFP^-PI^-. Sorted cells were lysed, and equal protein input was used to measure VEGF levels (picograms) by ELISA. VEGF levels were normalized to secretion from 10^6 cells.

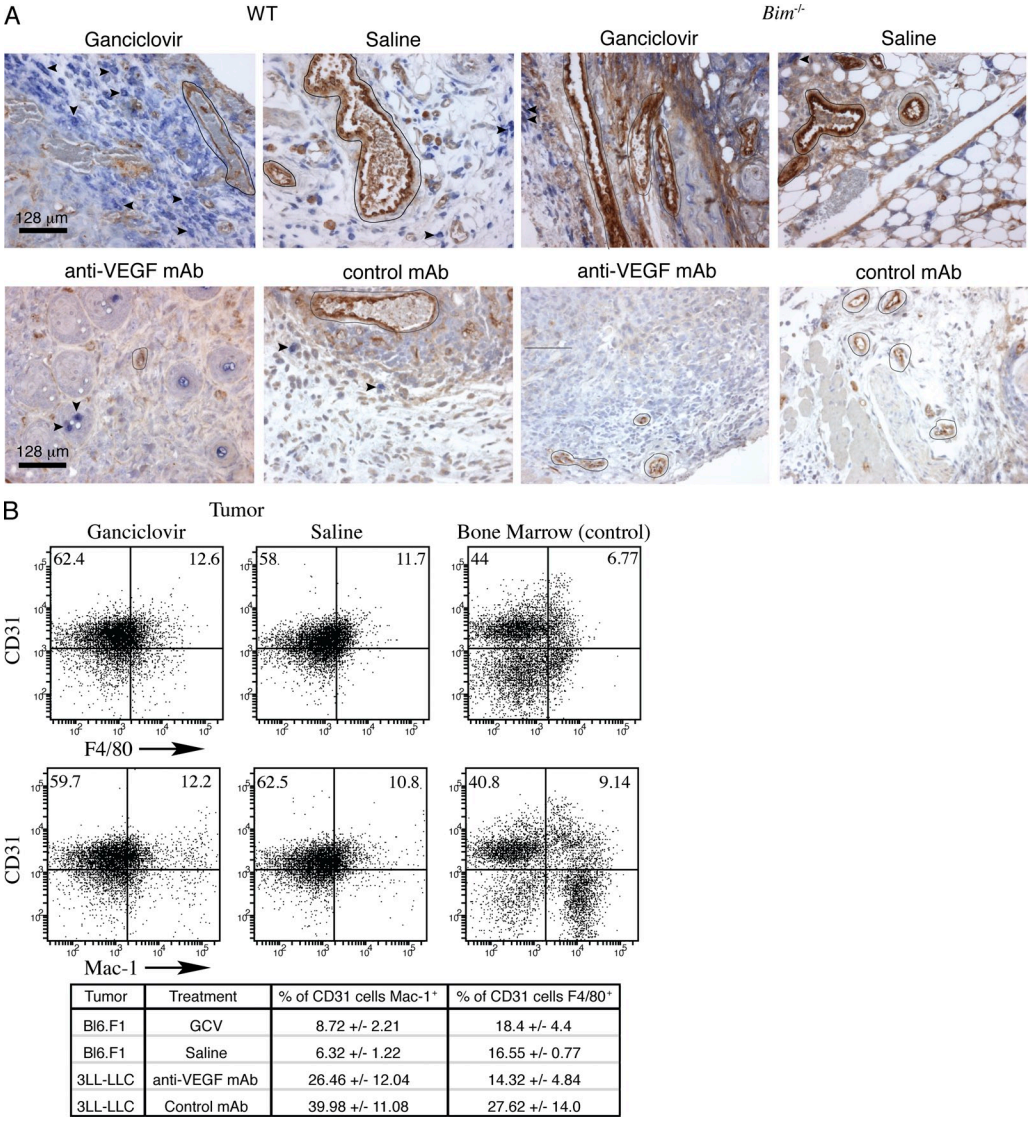

Tumor	Treatment	% of CD31 cells Mac-1$^+$	% of CD31 cells F4/80$^+$
Bl6.F1	GCV	8.72 +/- 2.21	18.4 +/- 4.4
Bl6.F1	Saline	6.32 +/- 1.22	16.55 +/- 0.77
3LL-LLC	anti-VEGF mAb	26.46 +/- 12.04	14.32 +/- 4.84
3LL-LLC	Control mAb	39.98 +/- 11.08	27.62 +/- 14.0

Figure S2. The majority of tumor-associated CD31$^+$ cells are not macrophages. (A) TK-expressing B16.F1 melanomas and 3LL-LLCs were grown subcutaneously in WT or *Bim*$^{-/-}$ mice until they reached a nominal volume of ∼50 mm^3, whereupon the animals received GCV (daily for 4 d), saline (control), anti-VEGF antibody (every second day for 1 wk), or Ig isotype–matched mAb (control) treatment. Data are representative of three independent mice per treatment group and genotype. Immunohistochemical staining of tumor sections was performed with antibodies to vWF (brown stain; which labels ECs, megakaryocytes, and platelets) and macrophages (F4/80; purple stain). Arrowheads indicate representative macrophages (purple staining), and fine lines surround endothelial structures (brown staining). (B) TK-expressing B16.F1 melanomas and 3LL-LLCs were grown subcutaneously in WT mice until they reached a nominal volume of ∼50 mm^3, whereupon the animals received GCV (daily for 4 d), saline (control), anti-VEGF antibody (every second day for 1 wk), or Ig isotype–matched mAb (control) treatment, respectively. Data are derived from analysis of 6 independent WT mice per treatment group (24 mice in total). The day after treatment was ceased, tumors were harvested, and samples were pooled to make three independent single-cell suspensions per treatment group and tumor type. These samples were stained for CD31$^+$, F4/80, and Mac-1. Representative flow cytometric analyses are shown, and the mean ± SD is represented in the table.

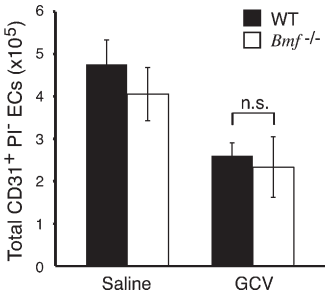

Figure S3. Absence of the BH3-only protein Bmf does not affect the survival of tumor-associated ECs after GCV treatment. B16.F1 melanomas were grown subcutaneously in WT or *Bmf*$^{-/-}$ mice until they reached a volume of ~50 mm^3, whereupon the animals were treated with GCV or saline. FACS analysis of single-cell B16.F1 tumor suspensions from saline- or GCV-treated WT or *Bmf*$^{-/-}$ mice was performed on day 4 (after three daily injections) to enumerate the viable tumor-associated ECs (CD31$^+$PI$^-$). Data represent the mean ± SEM (n = 5 per genotype and treatment condition). n.s., not significant.

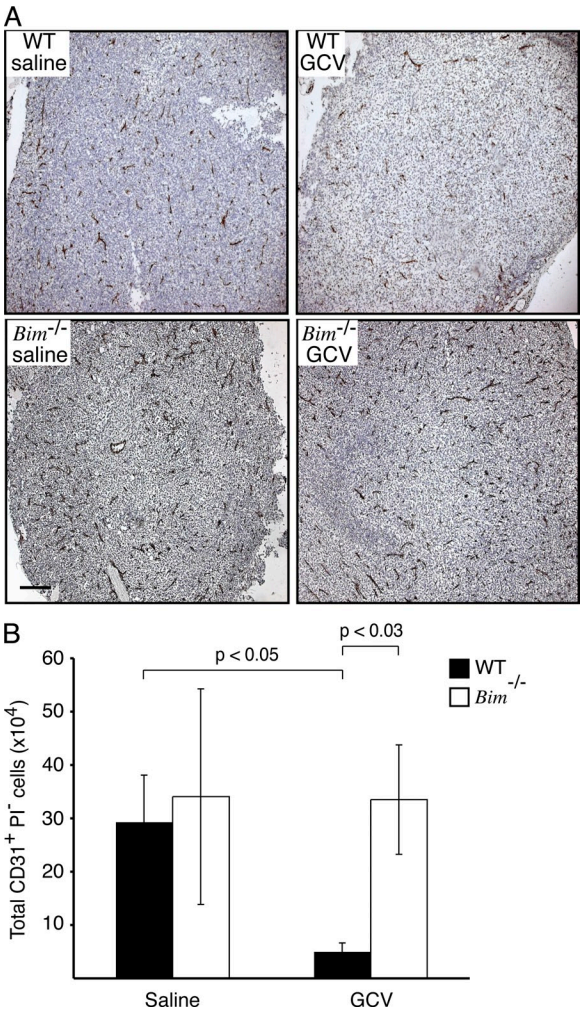

Figure S4. GCV-treated 3LL-LLCs grown in *Bim*$^{-/-}$ mice contain more viable tumor-associated ECs than those grown in WT mice. Saline or GCV treatment was initiated when 3LL-LLCs growing subcutaneously in WT or *Bim*$^{-/-}$ mice reached a nominal volume of 50 mm^3. Immunohistochemistry or immunofluorescent staining and FACS analysis were used to assess tumor vascularization. (A) Consistent with observations of B16.F1 melanomas (Fig. 2), three daily injections of GCV significantly reduced the number of CD31$^+$ vessels within 3LL-LLCs grown in WT mice. Bar, 200 mm. (B) The number of viable (CD31$^+$PI$^-$) ECs was significantly higher (P = 0.03) in GCV-treated tumors excised from *Bim*$^{-/-}$ mice than those found in tumors grown in WT controls. Data represent the mean ± SEM of five mice per genotype and treatment condition.

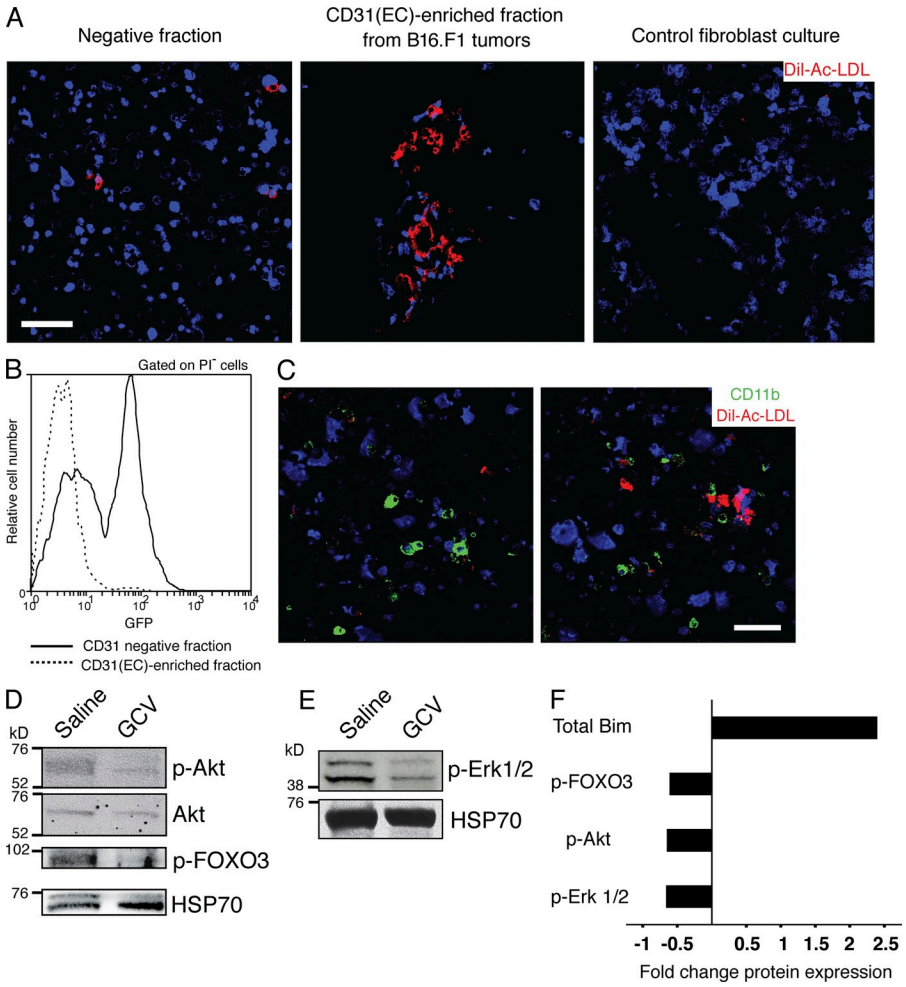

Figure S5. The PI3-K–Akt and MAPK–Erk1/2 signaling pathways are modulated in EC isolates from B16.F1 tumors. Single-cell suspensions of B16.F1 tumors were separated by anti-CD31 antibody staining and magnetic bead binding into a CD31$^+$ EC-enriched fraction and a fraction containing CD31$^-$ tumor cells plus tumor-associated stromal cells and fibroblasts. To evaluate their purity, cells in both fractions were assessed for the ability to internalize Ac-LDL, a property restricted to ECs and macrophages. (A) Representative confocal images show that the uptake of fluorescently labeled Ac-LDL was confined to the CD31$^+$ EC fraction, with little to no fluorescence signal in either the CD31$^-$ fraction or a WT E1A/*ras*-transformed mouse embryonic fibroblast cell line (negative control). Cells were counterstained with the nuclear dye DAPI (blue). (B) FACS analysis to assess whether the CD31$^+$ EC-enriched fraction was contaminated with GFP$^+$ tumor cells. The histogram from a representative purification demonstrates that GFP$^+$ tumor cells were not detectable within the CD31$^+$ EC fraction (dashed line) but abundant in the CD31$^-$ fraction (solid line). (C) Uptake of Ac-LDL is specific to ECs. Ac-LDL/CD11b double immunofluorescence staining confirmed that very few of the CD11b$^+$ cells present in tumor homogenates could incorporate Ac-LDL. (A and C) Bars, 40 µm. (D and E) The levels of phosphorylated (active) Akt, phosphorylated (active) Erk1/2, and phosphorylated (inactive) FOXO3a proteins were determined by Western blotting of tumor-associated ECs purified from B16.F1 melanomas grown in WT mice injected with saline (control) or GCV (as described in Fig. 3 C). Probing for total Akt and HSP70 served as loading controls. (F) Bar graph depicts densitometric analysis of the protein bands on the Western blots from Fig. 3 C and panels D and E using Quantity One image analysis software (Bio-Rad Laboratories). Values were normalized to loading controls, and fold-induction was calculated in comparison with levels observed in ECs from tumors excised from saline-treated mice.

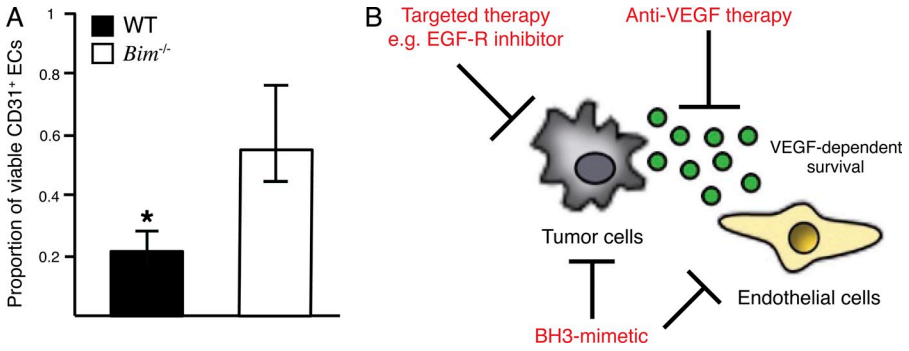

Figure S6. Bim deficiency protects intratumoral ECs from anti–VEGF antibody treatment in a de novo model of mammary carcinogenesis. (A) MMTV-PyMT transgenic mice were intercrossed with $Bim^{-/-}$ mice to generate MMTV-PyMT transgenic $Bim^{-/-}$ animals, which were compared with MMTV-PyMT $Bim^{+/+}$ (WT) animals. From 5 wk of age, mice were monitored twice a week for mammary adenocarcinoma development by palpation and caliper measurement. When tumors reached a calculated volume of between 100 and 200 mm^3, treatment with control IgG or anti-VEGF antibodies was commenced, and tumors were harvested on day 6. Data are depicted as the mean proportion ± SEM of viable ECs present in tumors from anti-VEGF antibody–treated mice in comparison with tumors from control IgG–treated mice of the same genotype ($n = 4$ for anti-VEGF–treated MMTV-PyMT transgenic $Bim^{+/+}$ and $n = 5$ for MMTV-PyMT transgenic $Bim^{-/-}$). *, P = 0.04 in comparison with the control IgG-treated MMTV-PyMT $Bim^{+/+}$ tumors. (B) Schematic representation of a combinatorial therapeutic approach to the treatment of solid tumors. Green circles represent tumor-derived VEGF.